Chapter 1

Highlights at ISOLDE

K. Blaum[a], M.J.G. Borge[b], B. Jonson[c], P. Van Duppen[d]

[a] *Max-Planck-Institut für Kernphysik, D-69117 Heidelberg*
[b] *PH- ISOLDE-PH, CERN CH-1211 Geneva-23*
[c] *Fundamental Physics, Chalmers University of Technology, SE-41296 Göteborg*
[d] *Instituut voor Kern- en Stralingsfysica, KU Leuven, B-3001 Leuven*

The ISOLDE Radioactive Bean Facility at CERN started fifty years ago as an interesting attempt to widen the palette of nuclear spices for experimental investigations. During this half century one has witnessed a steady development and refinement of the experimental programme. On the road towards the present day installation many scientific breakthroughs have been achieved. We present some of them here.

1. Introduction

The ISOLDE Radioactive Beam Facility is a dedicated installation at CERN for production and acceleration of radioactive nuclei. Isotopes from a variety of elements are produced in a target directly coupled to the ion-source of an isotope separator, which results in very short time-delay between production of an isotope and its occurrence in the experimental setup. Thus, the possibility to study isotopes out to the extremely short-lived ones at the limits of stability, is provided. The radioactive isotopes produced at ISOLDE are used in experiments in nuclear-, atomic-, solid-state and biophysics, as well in applications, particularly in medicine. The study of properties of nuclei all over the nuclear landscape gives not only clues to a detailed understanding of the structure of the nucleus but also about reactions in the Cosmos, where the chemical elements building up our Earth are born (Fig. 1).

2. Historical background

The pioneering experiment using an isotope separator directly linked to an accelerator was carried out in Copenhagen already in 1951.[1] Inspired of this, the European nuclear physics community proposed to build a general-purpose experiment for the production of short-lived isotopes connected to the synchro-cyclotron (SC) at CERN. The project was approved on December 17, 1964 by the CERN director Victor Weisskopf. An underground laboratory was built and protons from the SC

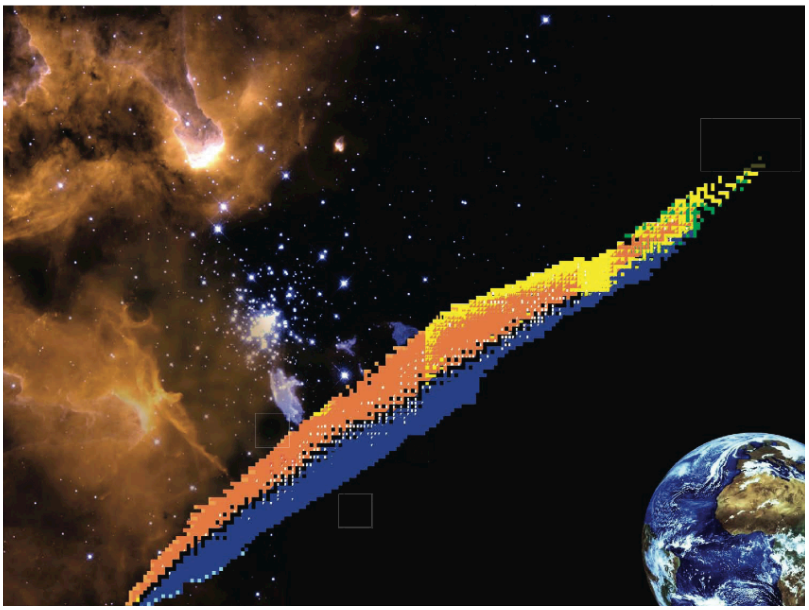

Fig. 1. The exotic nuclei studied at ISOLDE give important new insight in the complex nuclear many-body system. It gives clues to the simplicity hidden in the complexity, it tells us about the elements that build up the nature around us and about their cosmic origin and plays a prominent role in our understanding of the formation of the chemical elements.

were brought via a tunnel to hit a production target. The first experiment at this on-line isotope separator, named ISOLDE, was performed on September 17, 1967 (Fig. 14). ISOL has since then been the standard name for this type of radioactive isotope production method - the ISOL technique.

Just at the time of the first successful experiments at the new underground hall, CERN decided for a major upgrade of the SC. This SC improvement programme aimed at an increase in the internal beam intensity with a factor 10, to 10 μA , and an improved extraction efficiency giving ISOLDE a proton beam intensity increase of more than a factor 100. An essential part of the upgrade was to change the frequency system at the SC, which had been based on a tuning fork, to a rotating condenser. In order to cope with the higher proton current offered to ISOLDE an advanced technical development programme was launched. A new design of the target-ion-source systems was developed and, as it turned out, gave access to isotopes of more and more of the chemical elements. The SCIP program took place in the years 1972-74 and the new layout of the separator and its target-ion source became referred to as ISOLDE 2. The high intensity of produced isotopes and the large variety of different elements meant that ISOLDE had become a major international Facility to perform experiments on radioactive isotopes.

The SC machine had been in operation since 1957 and it became clear in the middle of the eighties that this accelerator had to be closed. To make the maximum

Fig. 2. The ISOLDE experimental hall in 1967. Note that ISOLDE at that time was part of the CERN Nuclear Chemistry Group, which meant white lab coats.

use of the last years of the SC the ISOLDE Collaboration proposed to build a second isotope separator. This new separator, ISOLDE 3, was constructed with a two-stage separation (one 90° magnet followed by a 60° one) to get very high resolution. A new target was placed in the SC vault and the produced radioactive isotopes were brought into the proton hall. The new separator gave a mass resolution of $M/\Delta M$ of 7000 and was a pre-runner for the design of the present High Resolution Separator (HRS) at the PS-Booster.

The future of the ISOLDE programme after the SC shutdown was discussed and the general consensus was that the most attractive option would be to move ISOLDE closer to the PS complex and to place its targets in an extracted 1 GeV beam from the PS Booster. The ISOLDE Collaboration set up a Technical Committee that helped CERN to find the optimal design of the new facility. A suitable layout was found and on May 4, 1990 the CERN Directorate approved the proposal to move ISOLDE to the PS Booster. The ground work for the new ISOLDE building started in October. At noon on December 19, 1990 the last shift of protons was delivered from the SC, almost exactly 26 years after the green light for ISOL experiments

Fig. 3. The ISOLDE experimental hall in 2007.

had been given from CERN.

The ISOLDE-PS Booster Facility was built in the usual CERN spirit and already in May 1992 the new installation could be inaugurated. The first experiment, a study of the beta decay of the two-proton halo nucleus ^{17}Ne,[2] was successfully competed on June 26 (Fig. 3).

The ISOLDE programme was traditionally mainly dedicated to study nuclear ground-state properties and excited nuclear states populated in radioactive decay experiments. With the large palette of different isotopes, produced in large quantities, it was an attractive possibility to build a post accelerator at ISOLDE. In 1994 such a proposal was presented to CERN asking for permission of the ISOLDE community to build a suitable accelerator to get exotic nuclear beams in the energy range 2-3 MeV/u. The project was approved and the REX-ISOLDE accelerator was built in an extension to the experimental hall. (See next section for details). The first beams were accelerated on October 31, 2001, and this addition to the ISOLDE programme has turned out to be both successful and very prolific.

3. Production, manipulation and acceleration of radioactive ion beams

The success of the ISOLDE facility is based on intertwined developments of radioactive ion beams (RIB) and instrumentation for physics experiments. The cross fertilisation lead to a broad spectrum of beams available with masses varying from ^{6}He to ^{232}Ra, with half lives in the ms region (e.g. ^{14}Be $T_{1/2}$=4.45 ms), intensities up to the nA level (e.g. ^{213}Fr with $\sim$8.10^{9} particles per second) and energies from rest to a few MeV/u.[3,4] A continuous development program implementing new techniques, like e.g. the use of nano-structured target material, laser resonance

ionisation, ion cooling and charge state breeding, kept the facility at the fore front of RIB science ever since it was constructed. The RIB production and manipulation process adapts the beam properties to the different experimental set-ups. As one mainly deals with short-lived radioactive isotopes that are produced in minute quantities compared to the vast amount of unwanted species produced (ratios over 10^{12} between the production rate of the unwanted versus wanted isotopes are routinely reached) the overall RIB production process has to be efficient, fast and selective.

3.1. *The target-ion source system – the heart of the matter*

ISOLDEs radioactive isotopes are produced in high energy proton induced reactions impinging on different target materials. The primary proton beams from CERNs PS Booster induce spallation, fragmentation and fission reactions which allow, by a proper choice of the target material, to produce a range of isotopes that covers a substantial part of the chart of nuclei below uranium (Z=92). As the reaction mechanisms are barely selective the target-ion source system producing the low-energy ion beam combined with the mass analysing magnet and other ion manipulation devices are used to reduce the unwanted contaminants and/or identify the isotopes of interest. Pioneering work to integrate the target and the ion source in one compact system that is kept at high temperature to speed up the diffusion and effusion of the radioactive atoms from the target container[3] led to a successful design that today is still competitive and that allows using different atomic and chemical processes to purify the beam. A simple but effective approach is cooling the transfer line between target and ion source, allowing only the gaseous elements (noble gases) or volatile molecules to reach the ion source. The reduction of elements that make a chemical bonding with the surface of quartz line installed between target and ion source represents another approach. Recently new routes towards more performing target materials that include the use of nanostructured target material are explored to reduce the delay time and for obtaining more ruggedised systems.

ISOLDE s successful laser spectroscopy programs and the fact that powerful pulsed laser systems became available lead to the implementation of laser resonance ionisation for the production of RIB in the beginning of the 90's. This element selective and efficient ionisation process combined with mass separation results in pure beams and the first on-line production of photo ionised radioactive Yb beams was soon followed by isotopes from a wide range of different elements.[5] Now the laser ion source is routinely used for over 50% of ISOLDE's beam time. A recent addition to the RILIS selectivity is the Laser Ion Source Trap (LIST) approach that integrates a standard target ion source system, laser ionisation and ion manipulation. It is based on photoionisation of the plume of atoms escaping from the high temperature ISOLDE target-ion source system, subsequent capturing of the ions in a radio-frequency trap and transporting them to the extraction region. While losses in overall efficiencies are encountered LIST improves the selectivity by about four orders of magnitude.[6]

3.2. *Cooled beams, isomeric beams and in-source laser spectroscopy*

Adapting the longitudinal and transverse RIB emittance or the beam pulse characteristics to the needs of the experiments was pioneered at ISOLDEs high precision mass spectroscopy set-up ISOLTRAP. The potential of buffer gas cooling in radio frequency or in Penning traps to produce cooled, bunched radioactive ion beams with good efficiency could be demonstrated. Larger versions of both the radio frequency ion trap and of the Penning trap were developed to deliver cooled and bunched beams to other ISOLDE users like the collinear laser spectroscopy set up, where it increased the peak-to-background ratio by two orders of magnitude and the REX-ISOLDE post-accelerator respectively (see section 3.3).

Soon after the first laser ionised RIB, isomeric beams were produced using the hyperfine splitting of the atomic transition.[7] Combining this isomer selectivity with β-decay and mass spectroscopy studies lead to the discovery of three β-decaying isomers in ^{70}Cu (see Fig.4) which could be explained as the coupling of one proton and one neutron to a ^{68}Ni core. With ISOLDEs post-accelerator (see section 3.3.), isomeric beams were post-accelerated and used for Coulomb excitation measurements probing the strength of the Z=28 shell and N=40 subshell closures.[8] This pioneering experiment moreover showed the triggered depopulation of a nuclear isomer using Coulomb excitation and called for a detailed study of other spin-multiplets in odd-odd nuclei.

Because of the high sensitivity of the laser ion source, in-source laser spectroscopy measurements with weak beams (intensities down to less than one atom per second) became possible but they were mainly limited to heavy mass nuclei because of the limited spectral resolution of the method. Charge radii and electromagnetic moments of a number of neutron deficient nuclei around the lead isotopes (Z=82) were obtained extending the pioneering work on optical spectroscopy of the mercury isotopes using samples from ISOLDE? (see section 4). This technique allowed to determine the unknown ionisation potential of astatine, the only element in the table of Mendelev below uranium for which this fundamental atomic property was not known experimentally. The result benchmarks quantum chemistry calculations and has an impact on the field innovative medical radioisotope production as the isotope ^{211}At, because of its decay properties, is an interesting pharmaceutical radioisotope for targeted alpha therapy in cancer treatment provided its chemistry is well understood. Building further on ISOLDEs know-how in RIB production and on CERNs proton beam capabilities, the CERN-Medicis (Medical Isotopes Collected from ISOLDE) was initiated. Medicis will exploit targets installed at ISOLDEs beam dump position and produce long-lived radioisotopes for fundamental studies in cancer research, for new imaging and therapy protocols and for pre-clinical trials.

The large variety of RIB with different decay properties and from various elements makes them tailored probes f or condensed matter and biophysics studies. The very low concentrations of radioactive impurity atoms in materials, surfaces or interfaces can be detected providing unique nanoscale information (see Fig. 5).

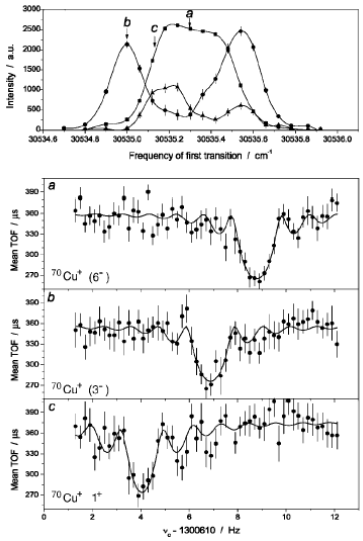

Fig. 4. Isomer selection is performed using the hyperfine splitting of the atomic levels probed in the resonant laser ionisation process used in the ISOLDE laser ion source. The yield of the different isomers in ^{70}Cu as a function of laser frequency is shown for the (6^-) (squares), (3^-) (circles) and 1^+ (triangles) β-decaying isomers of ^{70}Cu (top). The modified cyclotron frequency resonance spectra obtained at ISOLTRAP for three different laser frequencies (a, b and c) evidence the presence of three different isomers and allow to measure their mass whose difference is in perfect agreement with β-spectroscopy studies (bottom). The spectrum in (c) was obtained after an extra purification step in the Penning trap.

3.3. *REX ISOLDE – a new concept for post-acceleration of radioactive ion beams*

In order to broaden its physics scope and triggered by the successful post-acceleration of light RIB at the Louvain-le-Neuve (Belgium) project [9], new ways to accelerate the singly charged RIB in a universal, fast, efficient and cost-effective way were explored. This resulted in a novel concept based on ion beam cooling and bunching in the buffer gas of a Penning trap, charge-state breeding in an Electron Beam Ion Source (EBIS) and post-acceleration in a room-temperature linear accelerator. Ion beam cooling and bunching transferred the RIB from ISOLDE into bunches suited for injection in EBIS and was based on the ISOLTRAP experience. The efficient injection of singly charged ions in and extraction of highly charged ions from the EBIS was based on a concept from the Manne Siegbahn Institute (Stockholm, Sweden). Finally, the room temperature accelerator cavities were based on designs from the Max-Planck Institute for Nuclear Physics (Heidelberg, Germany).

While the original goals of this Radioactive beam EXperiment at ISOLDE REX ISOLDE project[?] (Fig. 6) were limited to energies up to 2 MeV/u and masses below A=50, the concept proved to be very successful and meanwhile beams with A/Q ratio <4.5 with masses up to 220 have been accelerated up to 3 MeV/u. Most of

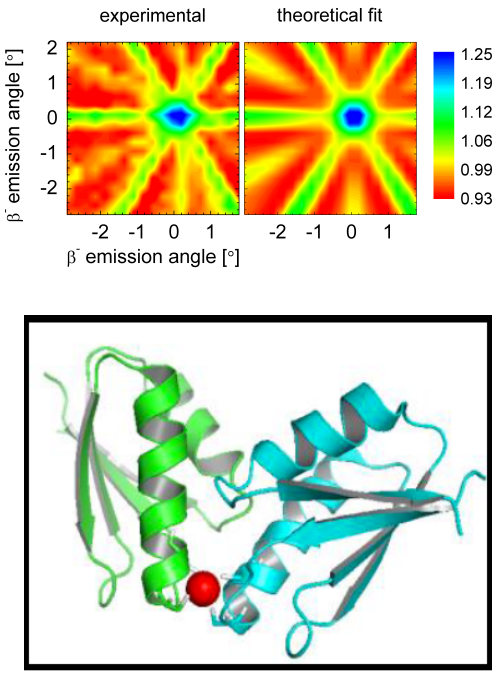

Fig. 5. Upper: Emission channeling data recorded using a position sensitive silicon detector. The colour scale corresponds to the angular dependent yield of channeled beta particles emitted from radioactive ^{56}Mn probes implanted into a GaAs (semiconductor) sample.[9] The data are fitted to simulations from which the site location of Mn in the GaAs matrix can be determined enhancing the understanding of electrical, optical and magnetic influence of dopants in semiconductors Lower: an artist impression from quantum chemistry calculations of a heavy metal ion binding protein. The position of the heavy metal, a radioactive Cd probe in this case, was determined by perturbed angular correlation measurements.

the beams have been used for Coulomb excitation measurements or few-nucleon transfer reactions using a dedicated particle and gamma-ray detector array for low-intensity low-multiplicity RIB experiments (Fig. 7). A major upgrade of the REX-ISOLDE facility, whereby the room temperature cavities will be replaced by super conducting ones and which will result in final beam energies up to 10 MeV/u for all ISOLDE beams, is currently ongoing. First beams from the High Intensity and Energy ISOLDE (HIE ISOLDE) are expected in 2016.

4. Nuclear shapes

Atomic nuclei exhibit single-particle and collective degrees of freedom. Understanding the delicate balance between these two extremes underpinning the structure of atomic nuclei is a challenge for theory. In general 'single-particle effects dominate the structure of nuclei at and around closed proton and neutron shells, while defor-

mation is observed in nuclei situated on the nuclear chart in between doubly closed shell nuclei. Shapes have been studied at ISOLDE using laser spectroscopy and Coulomb excitation measurements. While the former method results in charge radii, magnetic dipole and electrical quadrupole moments of ground states and long-lived isomeric states, the latter allows to obtain quadrupole moments and quadrupole or higher order transition strengths excited states. Throughout the nuclear chart experimental evidence has been accumulated for a phenomena called shape co-existence whereby quantum states with different deformation but similar binding energy appears at low energy in the nucleus. In the heavy nuclei it was discovered at ISOLDE serendipiously in the light mercury isotopes in optical spectroscopy measurements.[10] The strong staggering in the charge radii for the lightest mercury isotopes (see Fig. 8) was interpreted as due to the appearance in the odd-mass mercury isotopes of a strongly deformed ground state co-existing with a more spherical isomeric. The in-source laser spectroscopy data obtained in the neighbouring lead and polonium isotopes[12,13] combined with Coulomb excitation measurements in this region using the post-accelerated REX beams allowed to deduce the oblate nature of the ground-state deformation and supported the proposed interpretation of shape coexistence i nduced by particle-hole excitation across the closed proton shell.

The prevalent shape of nuclei is reflection symmetric quadrupole deformation but in some heavy unstable nuclei circumstantial evidence for octupole deformation has been reported. This type of reflection-assymetric or pear shaped deformation is not only important to test nuclear models, but isotopes exhibiting this type of

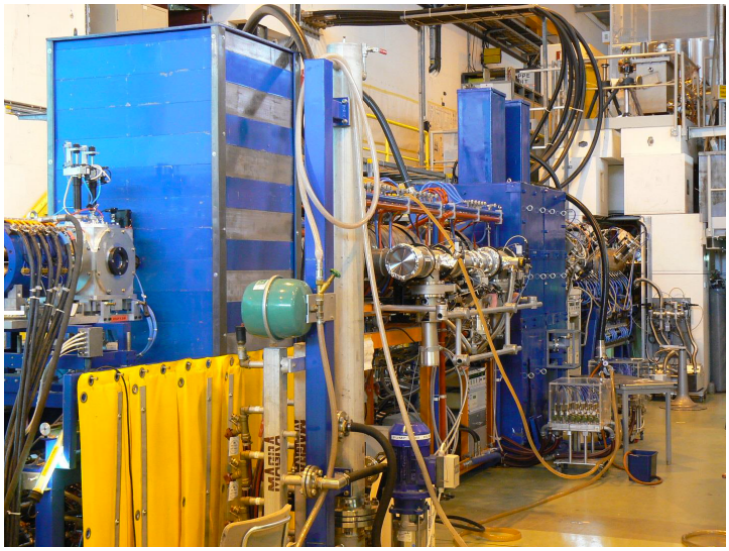

Fig. 6. The REX-ISOLDE post-accelerator delivering radioactive ion beams from ^{8}Li to ^{224}Ra with energies up to 3 MeV/u.

Fig. 7. The Miniball germanium detector array, developed for low-intensity RIB experiments, is shown in its retracted position. The germanium detectors surround a set of segmented silicon detectors that are placed in closed geometry in the spherical reaction chamber.

deformation are ideal probes to look for physics beyond the standard model. For the search of an atomic electric-dipole moment in odd-mass isotopes, static electric octupole deformation of the atomic nucleus amplifies the sensitivity by several orders of magnitude. In a recent Coulomb excitation experiment using energetic beams of ^{224}Ra, enhanced octupole deformation was evidenced through the measurement of octupole transition strengths (see Fig. 9).[14] This constrains suitable isotopes for studies of the atomic electric-dipole moments.

5. Nuclear halos

A considerable fraction of the experimental programme at the ISOLDE Facility concerns studies of beta decay, which is a well-proven probe of nuclear structure as well as of weak interactions (see Section 6). There is an important difference between beta-decay of near stable nuclei and those those in the drip-line regions. Close to stability the transitions occurs between discrete bound levels while the decay closer to the drip-lines also involves states in the continuum. In the neighbourhood of the drip-lines one also encounters beta-delayed particle emission processes, which in many nuclei dominate over decays to bound states.[15] A quite spectacular example of a beta-delayed particle precursor is provided by the last particle-bound lithium isotope, ^{11}Li. This nucleus has a beta-decay Q value, *i.e.* the mass difference between mother and daughter nuclei, of 20.623 MeV, while the neutron separation energy of its daughter, ^{11}Be, is as low as 504 keV. This energy unbalance opens up several possible beta-delayed particle emission channels, as illustrated in Fig. 10. In

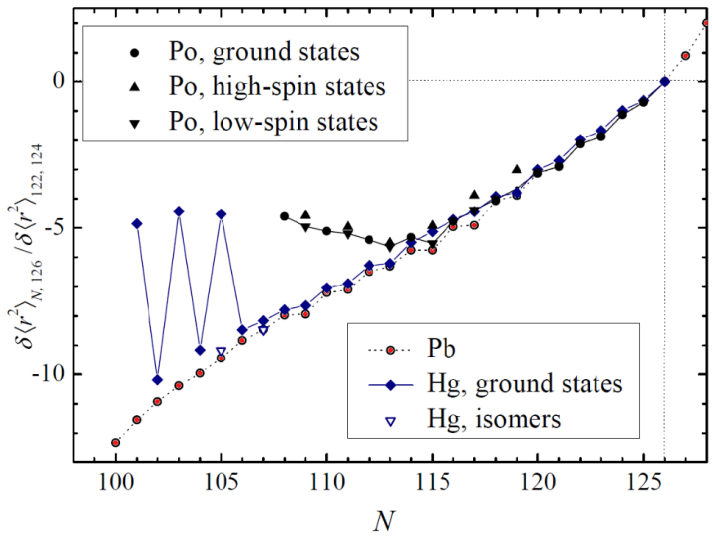

Fig. 8. Relative $\delta < r^2 >$ for the even-Z $_{80}$Hg (bleu), $_{82}$Pb (red) and $_{84}$Po (black). While the change in charge radii of one isotope compared to its neighbour for the heaviest isotopes are very similar for these three elements, large differences are observed further away from the N=126 neutron shell closure. The large staggering observed in the charge radii Hg data is interpreted as shape coexistence caused by the occupation of specific single-particle states. The deviation observed for the Po isotopes is linked to an onset of collective behaviour possibly caused by the same mechanism. Adapted from[13]

a number of experiments at ISOLDE at the end of the seventies and the beginning of eighties the observations of beta-delayed two-neutron, three-neutron and triton emission were observed for the first time.

Just at the time when the study of ^{11}Li was in focus at ISOLDE a group at Berkeley led by I. Tanihata[16] studied interaction cross-sections of Li isotopes. The remarkable result of this experiment was a large and abrupt increase in the matter radius for just ^{11}Li. Scientists working with lithium at ISOLDE came with an explanation for the increase of the radius based on the low two-neutron separation energy.[17] A model, where ^{11}Li should have a novel type of structure, a halo, was proposed. The basic idea is that the ^{11}Li nucleus is built up by a ^{9}Li core surrounded by two loosely bound neutrons forming a veil of neutron matter around the core.

The realisation of the occurrence of halo structure at the drip-lines sparked off an intense experimental activity and many nuclei having neutron and proton halos are known today.[18] Important early ingredients for the understanding of the halo structure came from ISOLDE where the spin, magnetic moment and the electric quadrupole moments were measured for the chain of bound Li isotopes in a combination of optical and beta-decay measurements,[19,20] results that later were confirmed and improved.[21] The results showed that the magnetic dipole and the electric quadrupole moments of the two isotopes ^{9}Li and ^{11}Li are very similar. This

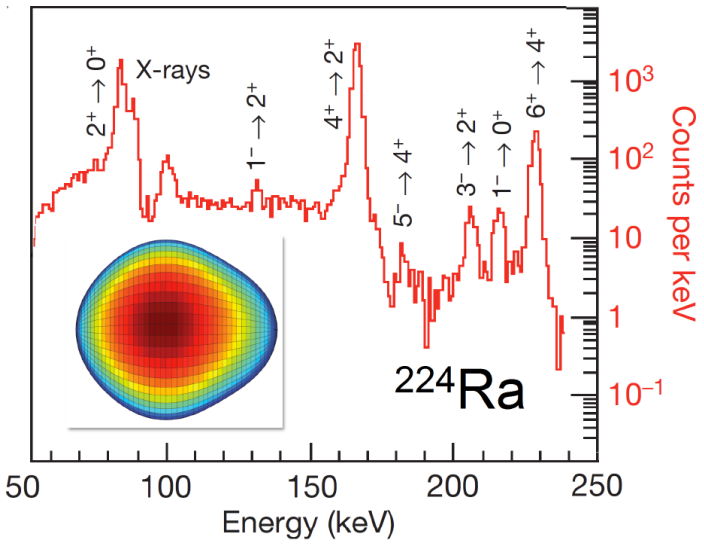

Fig. 9. Part of the gamma-ray energy spectrum obtained after Coulomb excitation of ^{224}Ra. From the intensities of the gamma-rays (indicated with the spin and parity of initial and final state), especially the ones de-exciting negative parity states, information on the octupole transition strength was deduced evidencing enhanced octupole deformation. The inset shows the static octupole deformation of ^{224}Ra in the intrinsic frame as deduced from the experiment.

proves that the increase in the radius arises from the neutron tail, while the charged core is little affected.

Another consequence of the two-neutron halo structure is the occurrence of beta-delayed deuteron emission. The Q value for this process is $Q(\beta^-\mathrm{d}) = 3.007$ - S_{2n} MeV.[22] The occurrence of this decay mode was shown at ISOLDE for the first time for the two-neutron halo nucleus ^{6}He[23] and later also for ^{11}Li.[24]

The beta-decay daughter of ^{11}Li is ^{11}Be, which is an example of a one-neutron halo nucleus. Its magnetic moment was measured at ISOLDE in a very beautiful experiment.[25] The Be isotopes are produced in a UC_2 target matrix irradiated by 1 GeV protons from the PS Booster Section3.1. The produced Be evaporate into a tungsten cavity, where two laser beams excite the atoms from the $2s^2\ ^1S_0$ atomic ground state to an auto-ionising state via the atomic $2s2p^1P_1$ state. The ^{11}Be$^+$ beam is then optically polarised by a collinear frequency-doubled CW dye laser beam. The polarised ions are implanted in a Be crystal placed in the centre of an NMR magnet. The first-forbidden beta decay to ^{11}B of the polarised nuclei are detected with two scintillators and the beta asymmetry is measured. From the observed Larmor frequency the magnetic moment is determined as $\mu(^{11}Be)$= -1.6816(8) μ_N. This value is confirming a 16 % core polarisation admixture in the ^{11}Be ground-state wave function.[26]

Another major experimental success was when the collinear laser technique was employed to determine the nuclear charge radii for Be isotopes. With a beam

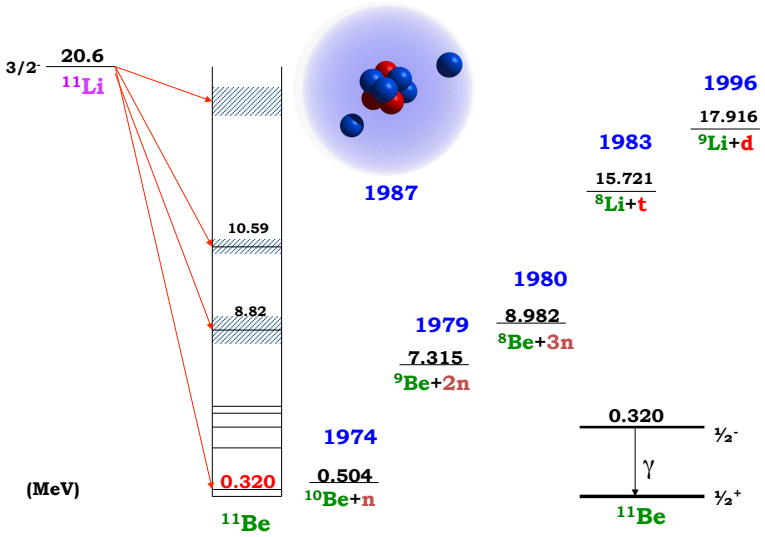

Fig. 10. The two-neutron halo nucleus ^{11}Li. The very high Q-value for beta-decay combined with the comparably low separation energies for various particles in the daughter nucleus ^{11}Be results in a multitude of different beta-delayed decay modes in this nucleus.

of Be^+ ions, a frequency comb and measuring the absolute transition frequencies for parallel and antiparallel geometry of the ion and laser beams, see Fig. 11, a hitherto impossible precision was obtained. The beauty of the technique is that the rest frame frequency, ν_0, is obtained independent of the acceleration voltage by combining the measured absolute transition frequencies for parallel (ν_p) and antiparallel (ν_a) laser beams so that $\nu_p\nu_a{=}\nu_0^2\gamma^2(1+\beta)(1-\beta) = \nu_0^2$. The required accuracy in the isotope shift measurement of 1 MHz was obtained. The charge radii were observed to decrease for the isotopes ^{7}Be to ^{10}Be and then increase for ^{11}Be, see Fig. 11.[27] This increase of the charge radius is expected since the centre of mass and the centre of charge does not coincide in the one-neutron halo nucleus for ^{11}Be Fig.11.

6. Fundamental studies

Radioactive beams are ideal probes for fundamental studies of weak interaction and of the Standard Model (SM) in general. Among others, precision measurements of masses, half-lives and branching ratios of superallowed β-emitters allow in combination with nuclear theory a precise determination of the first (V_{ud}) element of the Cabibbo-Kobayashi-Maskawa (CKM) quark-mixing matrix, which relates the quark weak-inteaction eigenstates to the quark mass eigenstates assuming three

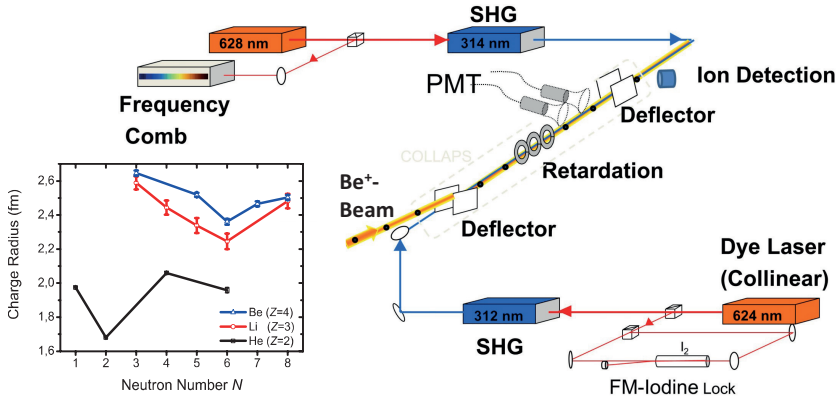

Fig. 11. Setup for collinear laser spectroscopy with parallel and antiparallel excitation and a frequency comb for reference for the determination of the charge radius for Be isotopes. The inset shows the state of the art of charge radii measurements[28] for light drip line nuclei.

quark generations. Taking V_{us} and V_{ub} from particle physics data, a stringent top-row unitarity test of the CKM matrix can be performed:[29]

$$\sum_j |V_{uj}|^2 = |V_{ud}|^2 + |V_{us}|^2 + |V_{ub}|^2 = 1. \quad (1)$$

Any deviation from 1 can be related to concepts beyond the SM such as the existence of an additional Z-boson or the existence of right-handed currents in the weak interaction. V_{ud} can be determined from the fundamental vector coupling constant G_V and the well-known weak-interaction constant G_F of purely leptonic muon decay: $V_{ud} = G_V/G_F$, where G_V in turns can be derived from the corrected strengths (Ft-value) of superallowed β-transitions, which are a function of the experimental parameters: decay Q-value, half-life $T_{1/2}$, and branching ratio b, as well as of different correction terms including isospin-symmetry-breaking and radiative correction. The uncorrected ft-values can be derived purely from nuclear physics experiments, namely from mass, half-life and branching ratio measurements of superallowed β-transitions. Many ISOLDE experiments, especially high-precision mass measurements with the Penning-trap mass spectrometer ISOLTRAP (see Fig. 12), being the first of its type installed at a radioactive ion beam facility in 1986, have contributed to this kind of research, providing the most accurate V_{ud} value to date of $|V_{ud}| = 0.974\,25(22)$.[29] Taking V_{us} and V_{ub} from PDG, one obtains the result:

$$|V_{ud}|^2 + |V_{us}|^2 + |V_{ub}|^2 = 1.000\,08(56), \quad (2)$$

i.e. the unitarity is fully satisfied to a precision of 0.06%.

Another pillar of the SM is the conserved-vector-current (CVC) hypothesis, saying that the vector part of the weak interaction is not influenced by the strong interaction.[?] Thus, Ft should be constant for all superallowed transitions. Taking

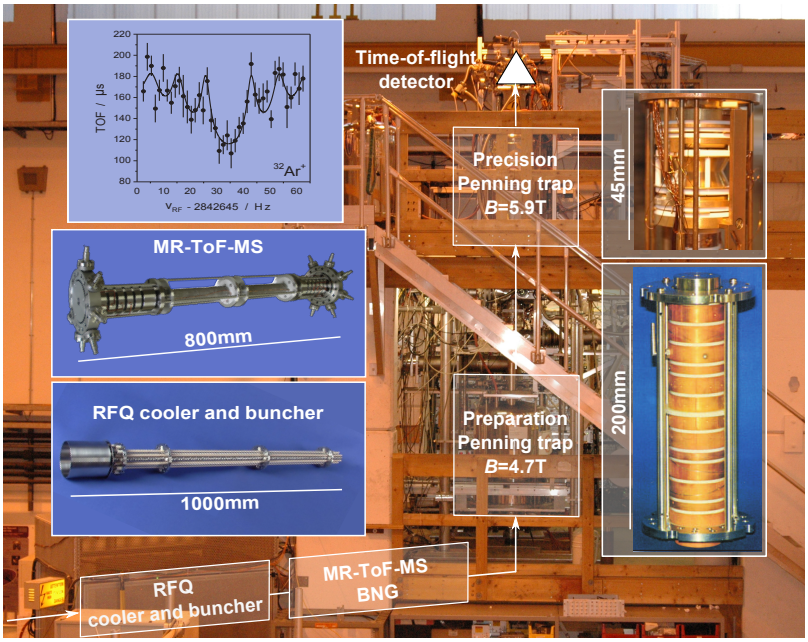

Fig. 12. Present setup of the ISOLTRAP Penning-trap mass spectrometer at ISOLDE for high-precision mass measurements on short-lived nuclides. The inset shows on the top left the cyclotron resonance of $^{32}Ar^+$ with the fit of the theoretically expected line-shape. The other insets show the different trapping devices at ISOLTRAP. At the time of the Ar measurement in 2001 the multi-reflection time-of-flight (MR-ToF) spectrometer was not installed at ISOLTRAP.

all presently available data results in an amazing consistency at the 0.03% precision level.[29]

Radioactive ions are also ideal systems to put constraints on scalar currents in weak interaction. One highlight example of ISOLDE are measurements on ^{32}Ar with a half-life of $T_{1/2} = 98$ ms. One of the best known value for the positron-neutrino correlation coefficient a was determined in the $0^+ \rightarrow 0^+$ β-decay of ^{32}Ar experiment at ISOLDE by Adelberger *et al.* in 1999.[30] The effect of lepton recoil on the shape of the narrow proton group following the superallowed decay was analyzed. Since the mass of ^{32}Ar was only known to an uncertainty of 50 keV at that time, the accuracy in the determination of a was limited to 6%. Thus, the mass prediction by the isobaric multiplet mass equation IMME was used instead and resulted in the beta-neutrino correlation coefficient for vanishing Fierz interference of $a = 0.9989 \pm 0.0052(stat) \pm 0.0039(syst)$ at the 68% C.L, thus being fully consistent with the SM prediction. Furthermore, a new limit on the masses of scalar particles with gauge coupling strength could be derived being at that time $M_S \geq 4.1 M_W$. A few years later the mass of ^{32}Ar was measured for the first time directly by Penning-trap mass spectrometry at ISOLTRAP/ISOLDE[31] (see inset of Fig. 12) with a mass uncertainty of only $\delta m = 1.8\,\mathrm{keV}/c^2$, thus allowing for an improved

value of a and relying no longer on the IMME prediction.

7. Shell structure: the decline of the magic numbers

The nucleus presents typical characteristics of few body and many-body quantum systems at the same time. Its microscopic and mesoscopic manifestation are governed by effective 2- and 3-body interactions of great complexity that depends not only of the distance between nucleons but also of its spins and moments.

In its macroscopic behaviour one observes properties equivalent to those of a liquid drop such as energy surface deformation, vibrations, rotations, shape transitions Experimental achievements related with these aspects are described in other section. Understanding of the arising of these semiclassical behaviours in terms of the quantum dynamics of the nuclear constituents, proton and neutrons, is one of the main challenges of nuclear theory.

In its microscopic behaviour the nucleus remind us to the atom as the fundamental ingredients are the orbitals and the interaction of individual nucleons, protons, neutrons or both. Experiments done with stable and near stable nuclei have shown that nuclei with N or Z equal to the so-called magic numbers 8, 20, 28, 50, 82 are more stables than their neighbours, supporting the use of the well established nuclear shell model. Maria Goeppert Mayer and J. Hans Jensen shared the Nobel price in 1963 for their independent development of the Shell Model in the year 1949 . The basic idea was that the complicated interaction of protons and neutrons in a nuclear system can be describe at zero order by a potential, spherical box that keeps them together, plus a very attractive spin-orbit interaction. This model could successfully explained the abrupt change in separation energy of the last proton and neutron of the nuclei with N or Z magic numbers. In this case the separation energy is maximal and it is followed by a strong drop for the neighbouring nuclei with N $\pm$ 1, Z or N, Z $\pm$ 1. Similar to the behaviour of the atomic ionisation energies around the noble gases. This model has been a success for the understanding of nuclear properties for stable or near stable atomic nuclei. The nuclei with magic numbers exhibit highly symmetric spherical configurations and are since then the milestones of the nuclear landscape. Although this model emerged from a pure phenomenological approach, modern nuclear theory can trace the magic numbers down to nucleon-nucleon forces derived from low-energy QCD. The advent of experimental facilities for the production of nuclei permitted to reach nuclei with a completely different balance between protons and neutrons, i.e. different isospin. It turned out that the traditional shell structure vanished in some regions of the nuclear chart, showing dramatic effects in the neutron rich side near the neutron binding limit, the neutron drip line, where the magic character appears at different, N or Z values. The persistence of the well defined shells near stability when going far away in regions with 'large imbalance of neutron and protons depends of the orbits near the Fermi level and on how large is the gap between shells. In another words the shell structure gets modified far from stability as the proton-

proton, neutron-neutron and proton-neutron interactions have different weight in the bounding nuclear potential.

States above the shell gap come down due to the pairing interaction (N=8) or quadrupole-quadrupole interaction and they are called intruder. In a extreme case these intruder states come below the Fermi level becoming the ground state contrary to the shell model predictions.

Many current studies of nuclear structure with exotic radioactive nuclei focus on the question of whether these magic numbers persist or are altered in going away from the valley of Stability. Challenging the predictive power of nuclear theory , the aim is to lead the way towards a universal description of nuclear structure. In this Chapter we will describe the CERN contribution to the discovery of the decline of the classic magic numbers that has slowly change the perception of the nuclear system and the relativity of the previous established knowledge.

Although the first anomaly in the expected order of nuclear orbits was observed in 1960 in ^{11}Be,[32] it was the measurement of the masses of the exotic sodium isotopes, ^{31,32}Na performed at CERNs PS that revealed a tighter bound than expected[33] nuclei. The excess of binding energy was associated with deformation and explained due to the excitation of neutron across the N=20 gap. These results were soon backup by the measurement of other ground state properties: spin, magnetic moments and mean charged radii.[34] Further the sodium beta-decay studies allowed for the determination of the first excited states of the magnesium isobars .[35] Also study at CERN. The data revealed that the N=20 isotopes had a sudden onset of deformation and thus a vanishing of the expected N=20 magicity. These neutron rich isotopes had a shell gap that it is not robust enough to avoid the excitations to higher shells developing quadrupole correlations that favour their deformation in the ground state. These results evidenced that certain terms of the nucleon-nucleon interaction changes for extreme isospin values. After these pioneering works many studies were dedicated to map and define the so-called island of inversion region where ^{32}Mg s situated in the centre.

The ground-state of ^{32}Mg is strongly deformed as shown from the large B(E2;$0^+_{gs} \rightarrow 2^+_1$) value, while the lighter even isotope ^{30}Mg shows a spherical 0^+ ground state with a deformed excited state 0^+ at 1788.2 keV which has a wave function with a strong intruder configuration. We called shape coexistence when a nucleus have states close in energy and with so different shape. This excited 0^+ state at 1788.2 keV has a wave function with a strong intruder contribution and was identified at ISOLDE by measuring the conversion electrons of the characteristic electric monopole transition between the two 0^+ states .[36] The existing ^{32}Mg data and theoretical predictions indicate that the levels in ^{32}Mg are inverted with the ground state deformed and composed of intruder configurations. The best prove of this assumption will be to identify a near-spherical excited 0^+ state, the analogue of the 0^+ ^{30}Mg ground state. In spike of several attempts this state could not be identified.

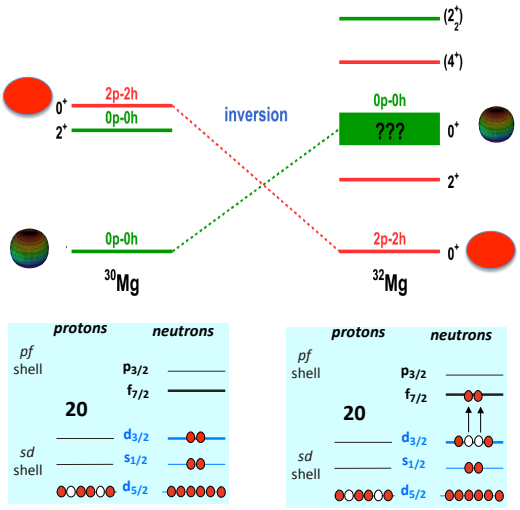

Fig. 13. The fascinating phenomenon of different nuclear shapes coexisting at similar energies the difference is less than 1 per cent of the total binding energy. It is the reduction of the N=20 shell gap that enables quadrupole correlations giving low-lying deformed $2p-2h$ intruder states from the fp shell to compete with spherical normal neutron $0p-0h$ states of the sd shell

A key idea was to add two neutrons to the spherical ground state of ^{30}Mg populating either the deformed ground state in ^{32}Mg or the excited spherical 0^+ in ^{32}Mg depending of which orbital the extra the neutrons will occupied. This was achieved at ISOLDE when a 1.8 MeV/u beam of ^{30}Mg ($T_{1/2}$=335 ms) was used to populate the ground-state and excited states in ^{32}Mg by a two-neutron (t,p) transfer reaction in inverse kinematics. An experimental challenge in this experiment was to produce the needed tritium target, which was done by loading tritium in a Ta foil. The detection of protons and gamma rays was done with the T-REX array and the MINIBALL Ge detector array. The T-REX is a 4π array consisting of a barrel of silicon-strip detectors together with an annular double-sided segmented silicon-strip detector of CD shape. Energy and position were measured for protons, deuterons and tritons. By studying angular distributions for the emitted protons one can determine the angular momentum transferred and from that the spin and parities of the states populated can be deduced. They could identify an excited state at 1058 keV excitation energy is a 0^+ state with spherical shape co-existing with the strongly deformed 0^+ ground state[37] . Such a low-lying and long-lived state poses challenges for currently established theory. The intruder states are of the 2-particles 2-holes type and benefit of a reduction of the N=20 gap to half of its value in the stable nucleus ^{40}Ca.

New magic numbers emerge far from stability giving rise to spectacular changes

Fig. 14. Here I could imagine an picture of the present ISOLDE with arrows pointing to the new buildings. For HIE it would be the hall extension. This needs, however, that we send up a brave man or woman in a crane for a nice photo. And maybe nice wether.

as it is the case of ^{34}Si, only two protons apart from ^{32}Mg that happen to be a double magic nuclei as in this case the gap of Z=14 is as important as the one corresponding to N=20. The intruder states are responsible of the vanishing of N= 8 shell in ^{12}Be which first manifestation was the level inversion observed in the one-neutron halo nucleus ^{11}Be, although in this case the pairing interaction is the one responsible for the strong correlations. The disappearance of the next magic number N=28 is due to the quadrupole-quadrupole interaction that lead to an equivalent shape transition when moving from the spherical N=28 isotones close to stability, to the predicted prolate shape of the near drip line nucleus ^{40}Mg (Z = 12, N=28). First experimental results published this year [38] seems to indicate that it is strongly deformed but more bound than expected. New experiments are designed with enhanced sensitivity to explore the behaviour and stability of heavier systems far from stability.

8. ISOLDE at the doorstep to the next half-century

In the period of writing this historic review of some of the landmark experiment we witness an intense period of completion of new projects for the future:

- The new post-accelerator structure HIE-ISOLDE
- The TSR storage ring
- The CERN-Medicis project.

References

1. O. Kofoed-Hansen and K.O. Nielsen, Phys. Rev. **82** (1951) 96;
   Kgl. Dan. Vidensk. Selsk. Mat. Fys. Medd. **26** (1951) No. 7.
2. M.J.G. Borge *et al.*, Phys. Lett. **B** 317 (1993) 25.
3. H.L. Ravn and B.W. Allardyce *in* Treatise on Heavy Ion Science, Vol. 8 (1989) 363.
4. P. Van Duppen and K. Riisager, J. Phys. G, **38** (2011) 1.
5. V. Mishin, *et al.*, NIM **B** 73 (1993) 550.
6. D. Fink *et al.*, NIM **B** 317 (2013).
7. U. Köster *et al.*, NIM **B**160 (2000) 528.
8. I. Stefanescu *et al.*, Phys. Rev. Lett. **98** (2007) 122701.
9. L. M. C. Pereira, *et al.*, Applied Physics Letters **98** (2011) 201905.
10. J. Bonn *et al.*, Phys. Lett. **B** 38 (1972) 308.
11. S. Decoster, U. Wahl *et al.*, Applied Phys. Lett. bf 97, 151914 (2010)
12. H. De Witte *et al.*, Phys. Rev. Lett. **98** (2007) 112502.
13. M.D. Seliverstov *et al.*, Phys. Lett. **B** 719 (2013) 362
14. L. Gaffney *et al.*, Nature **497** (2013) 202.
15. M.J.G. Borge, Phys. Scr. **T 152** (2013) 014013.
16. I. Tanihata *et al.*, Phys. Rev. Lett. **55** (1985) 2676.
17. P.G. Hansen, B. Jonson, Europhys. Lett. **4** (1987) 409.
18. K. Riisager, Phys. Scr. **T 152** (2013) 014001.
19. Arnold *et al.* Phys. Lett. **B** 197 (1987) 311.
20. Arnold *et al.* Phys. Lett. **B** 281 (1992) 16.
21. R. Neugart *et. al.* Phys. Rev. Lett. **101** (2008) 132502.
22. B. Jonson, K. Riisager, Nucl. Phys. **A** 693 (2001) 77.
23. K. Riisager *et al.*, Phys. Lett. **B** 235 (1990) 30.
24. I. Mukha *et al.*, Phys. Lett. **B** 367 (1996) 65.
25. W. Geitner *et al.*, Phys. Rev. Lett. **83** (1999) 3792.
26. T. Suzuki, T. Otsuka, A. Muta, Phys. Lett. **B** 364 (1995) 69.
27. W. Nörtershäuser *et al.*, Phys. Rev. Lett. **10** (2009) 062503.
28. K. Blaum, J. Dilling, W. Nörtershäuser, Phys. Scr. **T 152** (2013) 014017.
29. J.C. Hardy and I.S. Towner, Ann. Phys. **525** (2013) 443.
30. E.G. Adelberger *et al.*, Phys. Rev. Lett. **83** (1999) 1299 and
   E.G. Adelberger *et al.*, Phys. Rev. Lett. **83** (1999) 3101.
31. K. Blaum *et al.*, Phys. Rev. Lett. **91** (2003) 260801.
32. I. Talmi and I, Unna, Phys. Rev. Lett. **4** (2060) 469
33. C. Thibault *et. al.* Phys. Rev. **C 12** (1975) 644.
34. G. Huber *et. al.* Phys. Rev. **C 18** (1978) 2342.
35. D. Guillemaud-Mueller *et. al.* Nucl. Phys. **A** 426 (1984) 37.
36. W. Schwerdtfeger *et. al.* Phys. Rev. Lett. **103** (2009) 012501
37. K. Wimmer *et. al.* Phys. Rev. Lett. **105** (2010) 252501.
38. H. L. Crawford *et. al.* Phys. Rev. **C 89** (2014) 041303(R).